

Electron momentum distributions in graphite and diamond and carbon-carbon bonding

W. A. Reed, P. Eisenberger, K. C. Pandey, and L. C. Snyder

Bell Laboratories, Murray Hill, New Jersey 07974

(Received 1 April 1974)

A new measurement of the Compton profile of graphite is reported. These results, along with previously reported results for diamond, are compared with pseudopotential- and localized-bond-model calculations of the Compton profile. Qualitative but not quantitative agreement with experiment is obtained. We conclude that better band calculations are needed to achieve quantitative agreement and that a localized-bond model is reasonable for graphite.

I. INTRODUCTION

Much thought has been given to the degree of localization of electrons in chemical bonds and the extent to which the wave functions describing these bonds are transferable from one molecule to another.^{1,2} Hicks³ suggested that Compton scattering could provide this information about carbon bonds, and Eisenberger and Marra⁴ subsequently measured the electron momentum distributions of a series of molecular hydrocarbons. They found that a particular momentum distribution could indeed be identified with a particular carbon bond.

A related question is the extent to which the ground state of a solid is also describable by localized chemical bonds. Solid-state physicists have successfully developed band models to calculate the properties of solids but have tested their results primarily against the excitation properties of solids. These properties, however, tend to emphasize the delocalized excited states rather than the ground state. In this paper we make an initial attempt to answer the following questions: (i) How well do band models describe the ground-state properties in crystals, and (ii) to what extent can these ground-state properties be described by a localized-bond model? To evaluate the models we use the Compton profile, and in particular the anisotropy of the Compton profile, of a crystal. Reed and Eisenberger⁵ and Pandey⁶ have shown that the Compton profile is a sensitive test of the quality of wave functions generated by a given model. The solids which we consider are the two crystalline forms of carbon, diamond and graphite, since their properties can be most readily related to the properties of carbon in organic molecules.^{4,7}

Previous Compton measurements on diamond by Reed and Eisenberger⁵ indicate a distinct difference between the C-C bonds of diamond and ethane, which suggests the presence of solid-state effects in diamond. We further explore the nature of C-C bonding by measuring the electron momentum distribution in graphite. Although the electron momentum distribution of graphite has been previously measured by Compton scattering⁸⁻¹⁰ and by positron

annihilation,¹¹ the experimental data presented in these papers differ from the data presented here. The possible causes of these discrepancies will be discussed in Sec. II E.

Our measured Compton profile and anisotropy for graphite and our previously measured profile and anisotropy for diamond are compared with theoretical calculations which use pseudopotential, self-consistent-field (SCF) molecular, and SCF crystalline "Hartree-Fock" (SCHF) methods. A comparison of the various theoretical results with each other and with the data leads to some interesting observations which are discussed in detail in Sec. IV. The most salient observation is that the localized molecular model predicts the anisotropy of the Compton profile of graphite about as well as the pseudopotential method, although neither result is considered satisfactory. This result leads one to conclude that solid-state effects are minimal in the ground state of graphite. Comparison of the diamond data with theory seems to indicate that neither a tight-binding¹² (SCHF) nor a free-electron (pseudopotential) approach is able to predict the observed anisotropy of the Compton profile to the anticipated accuracy. Diamond seems to represent an intermediate case such that, starting from either of two extremes (free-electron or tight-binding models), one does not converge to an accurate solution. A model of diamond based on molecular wave functions does not work as well as the analogous model for graphite, indicating that more significant solid-state effects may exist in diamond.

II. EXPERIMENT

A. Compton scattering theory

The theory of the Compton scattering cross section and the validity of the impulse approximation have been previously described,¹³⁻¹⁵ so we will only list the important relations. From Ref. 15 we have

$$\frac{dJ}{d\Omega d\omega_2}$$

$$= \frac{r_0^2 m c \omega_2 \bar{X} J(q)}{2\omega_1 [(\omega_1^2 + \omega_2^2 - 2\omega_1\omega_2 \cos\theta)^{1/2} + (q/mc)(\omega_1 - \omega_2)]}$$

where (1)

$$\bar{X} = \frac{\omega_1(1+q/mc) + \omega_2(1-q/mc)}{\omega_2(1-q/mc) + \omega_1(1+q/mc)}, \quad (2)$$

$$q = \frac{(\vec{k}_1 - \vec{k}_2) \cdot \vec{p}_0}{|k_1 - k_2|}$$

$$= 137 \frac{\omega_1 - \omega_2 - \omega_1\omega_2(1 - \cos\theta)/mc^2}{(\omega_1^2 + \omega_2^2 - 2\omega_1\omega_2 \cos\theta)^{1/2}}, \quad (3)$$

$$J(q) = \int n(\vec{p}) dp_\alpha dp_\beta = \int |\chi(\vec{p})\chi^*(\vec{p})| dp_\alpha dp_\beta, \quad (4)$$

and

$$\vec{p}_\alpha \cdot \vec{k} = \vec{p}_\beta \cdot \vec{k} = \vec{p}_\alpha \cdot \vec{p}_\beta = 0. \quad (5)$$

Here we denote the energy and momentum of the incident and scattered photon by ω_1 , \vec{k}_1 and ω_2 , \vec{k}_2 , respectively, and $\hbar=1$. Our total profiles (including core) are normalized such that

$$\int_{-\infty}^{\infty} J(q) dq = 6 \text{ electrons.}$$

B. Experimental details

The basic experiment consists of scattering 159-keV γ rays from the sample, detecting the radiation scattered at 173° with a Ge(Li) detector, and recoding the signal on a multichannel analyzer. A description of the apparatus and data processing is contained in Refs. 5, 16, and 17.

The absolute value of the graphite Compton profile, averaged over all crystallographic directions, was measured on graphite powder. The powder was placed in a sample holder made by cutting a 2.54-cm hole in a 0.33-cm thick sheet of lead and covering this hole with 2.54×10^{-3} -cm-thick sheets of Mylar. The powder was packed in the holder such that its density was $\frac{1}{4}$ the density of the solid. Such a thin low-density sample was used to minimize the multiple scattering. To estimate the amount of multiple scattering, we also measured a powder sample 0.66-cm thick. Data were collected with the multichannel analyzer in the "add" mode until $\sim 24 \times 10^3$ counts appeared in the Compton peak, the powder was removed, and data again collected for an equal amount of time but with the analyzer in the "subtract" mode. The data both with and without the background subtracted were processed, which enabled us to check the consistency of our background and Mylar-window corrections.

Since large single crystals of graphite are not available, we were forced to use pyrolytic graphite to measure the anisotropy of the momentum distribution. Thus, we were only able to measure the distribution parallel to the c axis and the average

distribution normal to the c axis. The sample was $0.95 \times 0.95 \times 3$ cm with the c axis normal to the longest dimension, thus enabling us to measure the profile parallel and perpendicular to the c axis with identical geometry. The angular spread of the c axis was $\pm 0.4^\circ$. The large sample was used to increase the counting rate and 1.75×10^5 counts were collected in the peak for each direction. Although the multiple scattering effects are larger in this sample, we have shown⁵ that to first order the measured anisotropy is unaffected by multiple scattering as long as the geometry is constant.

The anisotropy data were processed in the manner described in Ref. 17. The profiles were first subtracted, averaged over $\pm q$, and then smoothed with a digital filter. The anisotropy data were not corrected for the resolution of the spectrometer since we feel that it is better to convolve the theory with our resolution function than to try to remove the effect of resolution from the data. Our resolution function is

$$R(q) = (1/\sigma\sqrt{2\pi}) e^{-[(q-q_0)/\sigma]^2/2}, \quad (6)$$

where $\sigma = 0.195$ a. u.

C. Experimental results

We processed the data before and after we electronically subtracted the effects of the background and Mylar windows and found that for $q < 2$ the profiles agree to better than 1%. We therefore list the average of the two sets of data in Table I. In columns 1–5 the $J(q)$ calculated from atomic wave functions for the $1s^2$ core¹⁸ and the valence profiles are listed. The data in columns 2 and 3 have had the effects of the instrumental resolution removed whereas the data in columns 4 and 5 are without resolution correction. The data in columns 3 and 5 are the result of extrapolating our data for the two thin samples to zero thickness. The errors listed represent our estimate of the sum of statistical and processing errors.

D. Anisotropy data

In Table II and Fig. 1 (solid curve) we present the difference between profiles taken parallel and perpendicular to the c axis uncorrected for the resolution of the spectrometer. The error bars are again our estimate of the statistical errors. As can be seen in the figure the electrons are more localized in the c direction, so that momentum is shifted away from $q = 0$ to $q > 1.8$ a. u.

E. Comparison with other experimental results

The only published data on graphite which gives numerical values for $J(q)$ are those of Weiss and Phillips.⁹ In general their averaged values agree well with ours, their value of $J(0)$ being about 1% lower. Their measured anisotropy is similar to

TABLE I. Measured compton profile of graphite.

| q (a. u.) | 1 ^a | 2 ^b | 3 ^c | 4 ^d | 5 ^e |
|-------------|----------------|----------------|----------------|----------------|----------------|
| 0 | 0.306 | 1.882 ± 0.015 | 1.898 | 1.834 ± 0.012 | 1.845 |
| 0.1 | 0.306 | 1.874 | 1.896 | 1.821 | 1.839 |
| 0.2 | 0.305 | 1.852 | 1.879 | 1.796 | 1.815 |
| 0.3 | 0.304 | 1.802 | 1.828 | 1.748 | 1.757 |
| 0.4 | 0.301 | 1.729 | 1.747 | 1.678 | 1.692 |
| 0.5 | 0.299 | 1.640 | 1.649 | 1.590 | 1.598 |
| 0.6 | 0.295 | 1.532 | 1.535 | 1.483 | 1.487 |
| 0.7 | 0.292 | 1.391 | 1.391 | 1.357 | 1.360 |
| 0.8 | 0.287 | 1.228 | 1.228 | 1.214 | 1.216 |
| 0.9 | 0.282 | 1.060 | 1.059 | 1.066 | 1.066 |
| 1.0 | 0.277 | 0.900 ± 0.009 | 0.894 | 0.918 ± 0.007 | 0.915 |
| 1.2 | 0.266 | 0.609 | 0.599 | 0.642 | 0.636 |
| 1.4 | 0.253 | 0.370 | 0.356 | 0.416 | 0.406 |
| 1.6 | 0.240 | 0.228 | 0.213 | 0.264 | 0.251 |
| 1.8 | 0.225 | 0.160 | 0.150 | 0.175 | 0.165 |
| 2.0 | 0.210 | 0.110 ± 0.004 | 0.105 | 0.119 ± 0.004 | 0.113 |
| 2.5 | 0.174 | 0.050 | 0.046 | 0.052 | 0.050 |
| 3.0 | 0.140 | 0.033 | 0.031 | 0.031 | 0.030 |
| 3.5 | 0.111 | 0.018 | 0.018 | 0.020 | 0.020 |
| 4.0 | 0.087 | 0.014 ± 0.002 | 0.014 | 0.014 ± 0.002 | 0.014 |
| 5.0 | 0.052 | 0.006 | 0.006 | 0.006 | 0.006 |
| 6.0 | 0.031 | 0.002 | 0.002 | 0.002 | 0.002 |
| 7.0 | 0.018 | 0.000 | 0.000 | -0.000 | -0.000 |
| 8.0 | 0.011 | 0.001 | 0.001 | 0.002 | 0.002 |
| 9.0 | 0.007 | -0.001 | -0.001 | -0.000 | -0.000 |

^aCarbon core profile from Ref. 18.

^bValence profile from 0.33-cm-thick powder sample corrected for spectrometer resolution.

^cValence profile corrected for multiple scattering and spectrometer resolution.

^dValence profile from 0.33-cm-thick powder sample. No resolution correction.

^eValence profile corrected for multiple scattering. No resolution correction.

ours but the large scatter in their data makes comparison with any calculation difficult.

Cooper and Leake⁸ present their data in unnormalized and graphical form so that it is not possible to directly compare our data with theirs.

The anisotropy data of Felsteiner *et al.*¹⁰ are also in major disagreement with our results. We believe that since they used a flat plate for a sample, the anisotropy they observed is dominated by multiple scattering and does not reflect the intrinsic anisotropy of the momentum distribution.

Although it is difficult to compare our work with the positron annihilation data of Berko *et al.*¹¹ it is interesting to note that they measure the maximum value of $J_{||c}$ at $q \sim 0.3$, which is similar to what is predicted by the theories. It is not surprising that they are able to observe the minimum at $J(0)$ while we cannot, since their resolution is several times better than ours.

III. THEORETICAL CALCULATIONS

One thing clearly lacking in the Compton scattering field has been a comprehensive comparison between theory and experiment. The work on diamond, silicon, and germanium⁶ shows that good agreement is obtained between the pseudopotential meth-

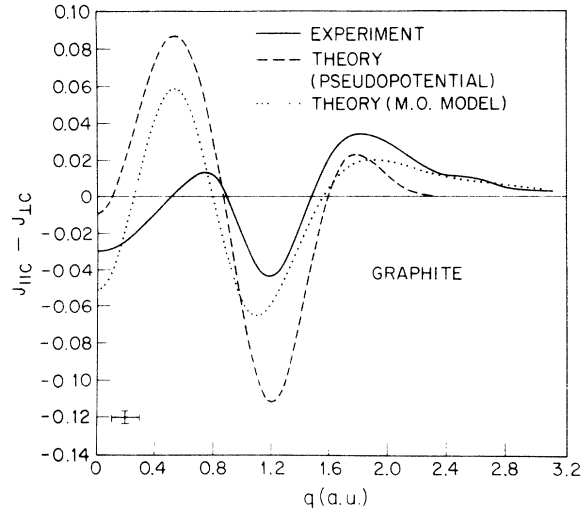


FIG. 1. Anisotropy of the Compton profile of graphite parallel and perpendicular to the c axis. Theoretical curves have been convolved with experimental resolution function.

od and experiment for silicon. For diamond, agreement is considerably poorer, which is to be expected since the pseudopotential approach has difficulty because there are no p states in the core of carbon. In this section three theoretical models and results will be described so that in Sec. IV we can compare the various models with experiment.

While a large number of energy-band calculations have been done for graphite,¹⁹ there still

TABLE II. Measured anisotropy of the compton profiles of graphite.

| $J_{ c} - J_{\perp c}$ | | | |
|-------------------------|------------|-----|------------|
| q | ΔJ | q | ΔJ |
| 0 | -0.028 | 1.7 | 0.028 |
| 0.1 | -0.025 | 1.8 | 0.032 |
| 0.2 | -0.021 | 1.9 | 0.034 |
| 0.3 | -0.017 | 2.0 | 0.032 |
| 0.4 | -0.006 | 2.1 | 0.026 |
| 0.5 | 0.003 | 2.2 | 0.020 |
| 0.6 | 0.008 | 2.3 | 0.016 |
| 0.7 | 0.011 | 2.4 | 0.013 |
| 0.8 | 0.010 | 2.5 | 0.012 |
| 0.9 | -0.002 | 2.6 | 0.010 |
| 1.0 | -0.020 | 2.7 | 0.006 |
| 1.1 | -0.037 | 2.8 | 0.004 |
| 1.2 | -0.042 | 2.9 | 0.003 |
| 1.3 | -0.035 | 3.0 | 0.002 |
| 1.4 | -0.018 | 3.1 | 0.001 |
| 1.5 | 0.002 | 3.2 | 0.001 |
| 1.6 | 0.019 | | |

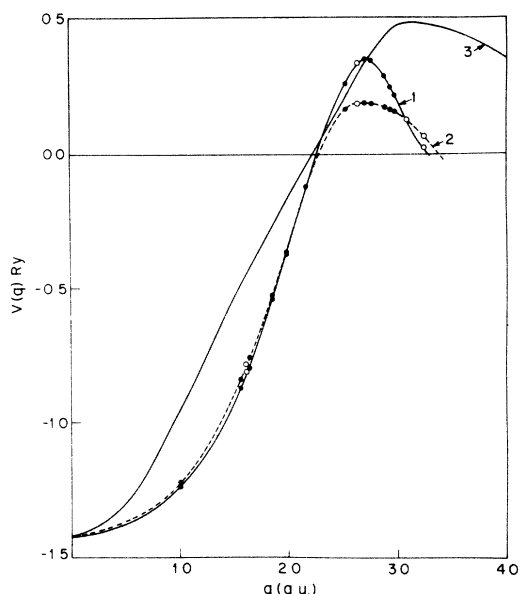


FIG. 2. Pseudopotential form factors used for graphite (●) and diamond (○). Curves 1 and 2 used in present calculations, curve 3 taken from Ref. 25.

exist considerable uncertainties in the interpretation of galvanomagnetic and optical experiments. All of these calculations are based on the tight-binding approximation, most of them ignoring the interaction between atoms in different layers. Further, most of these tight-binding calculations are empirical in the sense that the matrix elements of the Hamiltonian are treated as parameters and are obtained by fitting to experiments. Thus, the basis functions (localized atomic orbitals) in which the Bloch functions are expanded are not actually determined. Since the Compton profile depends on the ground-state momentum density, such parametrized energy-band calculations are of little value. In principle, one can start with atomic orbitals and perform a tight-binding calculation, but it is quite complicated.

A. Pseudopotential calculation

No such problem arises if the band calculations are done by the pseudopotential or OPW method. These are especially suited for the calculation of momentum density and hence the Compton profile. The pseudopotential method has been reasonably successful in interpreting optical data of diamond,²⁰⁻²³ where the pseudopotential parameters are determined empirically. Van Haeringen and Junginger²⁴ have used this method to calculate the energy bands of graphite. The potential parameters they used were obtained by scaling the results for diamond.²³ Their over-all results for graphite energy bands are in reasonably good agreement with experiment. However, the fine details,

particularly the overlap of the valence and the conduction bands, do not agree with the accepted interpretation of the galvanomagnetic data.

In spite of the uncertainties in the pseudopotential energy bands, it is interesting to determine if the calculated Compton profiles and especially the anisotropies between different directions are accurate. We have calculated the Compton profiles in three different directions: parallel to the a axis ($[10\bar{1}0]$), perpendicular to the a axis in the basal plane ($[11\bar{2}0]$), and parallel to the c axis ($[0001]$). The calculations were done in the single-particle approximation for two different sets of pseudopotential coefficients obtained from Refs. 22 and 23. The atomic pseudopotential form factors are shown in Fig. 2 together with the model potential of Animalu and Heine.²⁵ The calculation of the energy bands by the pseudopotential method is well known²⁶ and will not be discussed here. The details of the graphite structure are discussed in Ref. 19. Our results for both potentials are very similar and agree with those of van Haeringen and Junginger²⁴ to within 0.3 eV. Since both potentials yield essentially the same momentum anisotropy, the results we report here are those for the potential labeled 1 in Fig. 2.

The calculation of the Compton profile has been discussed previously^{6,27} so that we include here only the important relations and the modifications pertinent to the graphite structure. In the impulse approximation, the momentum density and the Compton profile $J(q)$ are related by

$$J(\vec{q}) = \int n(\vec{p}) (\vec{p} \cdot \vec{q} - q^2) d\vec{p}, \quad (7)$$

where $n(\vec{p})$ is the momentum density of electrons of the whole system in the ground state. In the single-particle approximation, the momentum density is given by

$$n(\vec{p}) = \sum_l \sum_{\vec{k}} \left| \int d\vec{r} \Psi_{l,\vec{k}}(\vec{r}) e^{-i\vec{p}\cdot\vec{r}} \right|^2 f(\mathcal{E}_{l,\vec{k}}), \quad (8)$$

where $\Psi_{l,\vec{k}}(\vec{r})$ is the single-electron wave function for an electron in the l th band for the wave vector \vec{k} inside the first Brillouin zone, and $f(\mathcal{E}_{l,\vec{k}})$ is the occupation of this state and is taken as the Fermi distribution. The sum over \vec{k} and l spans the occupied part of the Brillouin zone and the occupied band, respectively.

Once the electronic wave functions have been calculated, it is straightforward to calculate momentum density and Compton profiles using (7) and (8). The main difficulty arises from the sum over \vec{k} . Great simplification occurs if we ignore the overlap of the valence and conduction bands. As this overlap is well known to be small in graphite^{19,24} we will ignore this effect. This is further justified in view of the fact that the band structure in this region is quite uncertain. It

TABLE III. Theoretical Compton profile for valence electrons of graphite and benzene.

| q (a. u.) | Pseudopotential | | | MO model | | Benzene C-C bond |
|-------------|------------------------------|------------------------------|------------------------|-----------|---------------|---------------------|
| | $\langle 10\bar{1}0 \rangle$ | $\langle 11\bar{2}0 \rangle$ | $\langle 0001 \rangle$ | $J_{ c}$ | $J_{\perp c}$ | |
| 0.1 | 2.050 | 2.011 | 1.969 | 1.870 | 1.958 | 1.892 |
| 0.1 | 2.024 | 2.016 | 1.984 | 1.876 | 1.954 | 1.881 |
| 0.2 | 1.987 | 2.010 | 1.996 | 1.885 | 1.931 | 1.854 |
| 0.3 | 1.913 | 1.978 | 2.010 | 1.876 | 1.864 | 1.795 |
| 0.4 | 1.842 | 1.895 | 1.973 | 1.829 | 1.751 | 1.705 |
| 0.5 | 1.762 | 1.759 | 1.894 | 1.731 | 1.609 | 1.602 |
| 0.6 | 1.675 | 1.607 | 1.754 | 1.585 | 1.471 | 1.477 |
| 0.7 | 1.526 | 1.438 | 1.570 | 1.404 | 1.340 | 1.338 |
| 0.8 | 1.327 | 1.275 | 1.348 | 1.209 | 1.217 | 1.191 |
| 0.9 | 1.119 | 1.109 | 1.142 | 1.016 | 1.084 | 1.040 |
| 1.0 | 0.945 | 0.966 | 0.896 | 0.839 | 0.937 | 0.893 |
| 1.2 | 0.680 | 0.750 | 0.509 | 0.552 | 0.630 | 0.600 |
| 1.4 | 0.398 | 0.370 | 0.303 | 0.355 | 0.375 | 0.396 |
| 1.6 | 0.127 | 0.104 | 0.164 | 0.228 | 0.212 | 0.258 |
| 1.8 | 0.012 | 0.021 | 0.052 | 0.149 | 0.123 | 0.173 |
| 2.0 | 0.000 | 0.000 | 0.000 | 0.100 | 0.078 | 0.130 |
| 2.5 | | | | 0.044 | 0.055 | |
| 3.0 | | | | 0.024 | 0.034 | |
| 3.5 | | | | 0.014 | 0.020 | |
| 4.0 | | | | 0.009 | 0.009 | |
| 5.0 | | | | 0.004 | 0.004 | |

is estimated to give errors $\sim 1\%$ in the Compton profile at about the Fermi momentum. Also, since the momentum density $n(\vec{p})$ has the symmetry of the point group of the crystal, we need to consider only those \vec{k} which lie in the irreducible section of the Brillouin zone which has $\frac{1}{24}$ of the volume of the whole zone. Further, as shown in Ref. 6, the momentum density $n(\vec{p})$ is a smooth function so that only a relatively small number of \vec{k} points in the Brillouin zone need to be considered. In order to sum over \vec{k} vectors, we divided the Brillouin zone into smaller zones that have a shape identical to the Brillouin zone (i.e., hexagonal prism), such that the reciprocal vector along the $[0001]$ direction is divided into six equal parts and that along the $[10\bar{1}0]$ direction into 13. The wave function was calculated for the \vec{k} points at the centers of the smaller zones. This division leads to 63 \vec{k} points in the irreducible section and 1512 points in the full zone. Because of lower symmetry in graphite we need a larger number of \vec{k} points compared to diamond.⁶ In order to avoid interpolation, the calculation of the Compton profile in different directions was done only for those values of momentum (in the extended zone) that register with the above division in that particular direction.

The results for the calculated Compton profile for graphite are given in columns 1-3 of Table III as well as in Fig. 1 (dashed curve), where it is compared with experiment. In the figure, $J_{\perp c}$ is the average of the $[10\bar{1}0]$ and $[11\bar{2}0]$ directions and both $J_{||c}$ and $J_{\perp c}$ have been convolved with the resolution function. In this calculation the core orthogonalization effect has been completely ignored. It is a straightforward though tedious task to include

them in the way they were treated in diamond.⁶ We estimate²⁷ that this modification would lower the value of $J(0)$ by $\sim 5\%$ and correspondingly increase the profile for $q \gtrsim k_f$. However, it would not change the anisotropy. In view of the approximations and uncertainties in the pseudopotential form factor and the limitations of the numerical calculations, especially in the convergence of the wave function, the agreement with experiment is considered good.

For the purpose of later discussion the anisotropy of the Compton profiles for diamond as calculated by the pseudopotential method⁶ is shown in Fig. 4.

B. Molecular-orbital MO calculation

Electron wave functions in position space expanded in terms of Gaussian one-electron orbitals are particularly convenient for calculating Compton profiles since the wave function in momentum space is obtained by the Fourier transform

$$\chi(\vec{p}) = (1/2\pi)^{3N/2} \int e^{-i\vec{p}\cdot\vec{r}} \Psi(\vec{r}) d^3 r, \quad (9)$$

where N is the number of electrons. In addition, high-quality SCF wave functions are becoming available for many closed-shell molecules⁷ so it is of interest to see if this theoretical approach can predict Compton profiles and anisotropies.

One attempt has already been made by Cooper and Leake⁸ who used wave functions, calculated in the Huckel approximation,^{28,29} to calculate the Compton profiles for graphite parallel to the c axis and an average perpendicular to the c axis. Unfortunately, their calculation is in poor agreement with experiment since they find $[J_{||c} - J_{\perp c}] > 0$ instead of < 0 as measured. However, we believe that this error is probably a consequence of their using the same Slater exponent for all $2s$ and $2p$ functions on a carbon atom.

In this paper our objective is to employ *ab initio* wave functions for small molecules to construct a simple model for the Compton profile of graphite. The model we have chosen is a single valence-bond structure of the graphite sheet which consists

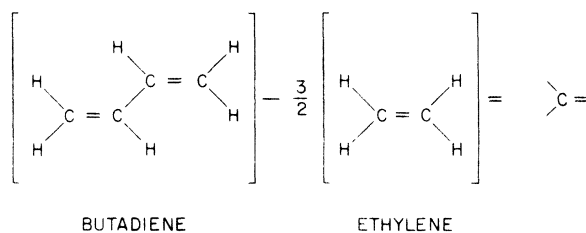


FIG. 3. Molecular model for graphite.

of one-half of a C-C π bond and three-halves of a C-C σ bond to the nearest-neighbor carbons and which neglects all resonance "solid-state" effects. We have modeled this fragment as transbutadiene minus $\frac{3}{2}$ ethylene, where the planes of the molecules are common and the C=C bonds are parallel. This model is illustrated schematically in Fig. 3. The c axis of graphite corresponds to a direction perpendicular to the planes of these molecules. The Compton profile J_{11c} for graphite is computed for this direction of the model system and normalized to four electrons. The Compton profile J_{1c} is taken as the mean of the profiles computed for directions in the molecular planes, parallel and perpendicular to the C-C bonds. The results for the calculated profiles are given in Table III, columns 4 and 5, and the anisotropy $J_{11c} - J_{1c}$ is shown in Fig. 1 (dotted curve). Again, the theory in the figure has been convolved with the resolution function.

A similar approach was used to obtain a molecular model for diamond and thus obtain the molecular Compton profile and anisotropy. In this case the C-C bond in diamond was modeled by taking the valence electrons of four ethane molecules oriented with their C-C bonds in the tetrahedral directions and subtracting the valence electrons of six properly oriented methane molecules. Although the average Compton profile is predicted rather well, this model fails to predict the observed anisotropy of diamond. A successful application of this model requires an equivalence of the C-H bonds of methane and ethane since their effect is to be removed by subtraction. It is possible that neopentane may provide a better molecular model since the carbon atom has the same tetrahedral coordination as in diamond. Wave functions for neopentane are presently being computed (by L. C. S.).

C. Crystalline SCHF calculations

As was mentioned in Sec. I, Wepfer *et al.*¹² have performed a self-consistent crystalline "Hartree-Fock" calculation of the Compton profiles of diamond using Gaussian orbitals as basis functions. The details of their calculation are found in Refs. 12, 30, and 31. In Figs. 4(a) and 4(b) we plot the anisotropy in their calculated profiles (smeared with our resolution function) for two pairs of directions.

IV. DISCUSSION

In Tables I and III we list the results of our experiment and theoretical calculations for graphite and compare these results graphically in Fig. 5. Each theoretical curve in this figure is the average of the crystallographic directions listed in the table. The average was then convolved and deconvolved with our resolution function for better com-

parison. We also list in Table III a profile appropriate for the C-C bond in benzene. This "benzene" profile was calculated by subtracting the appropriate C-H bond contribution⁴ from the measured benzene profile and normalizing it to four electrons. In Fig. 6 we compare this "benzene" profile to the measured profile for powdered graphite. In order to better illustrate the differences between the four profiles shown in Figs. 5 and 6, we have plotted in Fig. 7 the difference between our experimental graphite profile and the other three profiles. It should be noted that the agreement between the experimental benzene and graphite results is as good as either theoretical result is to the experiment. The main reason the pseudopotential results disagree with experiment is that core orthogonalization effects have not been included. In Fig. 1, where we compare the experimental and theoretical anisotropies, the striking feature is that the

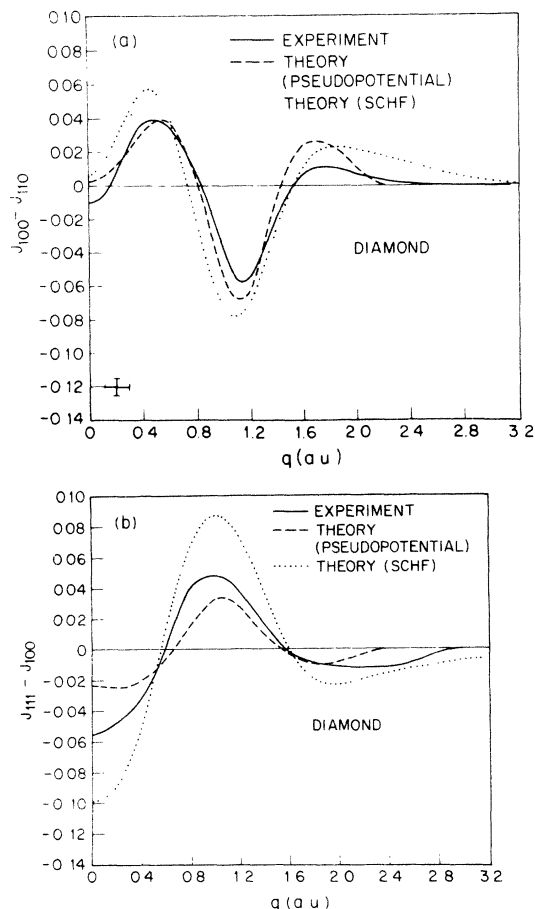


FIG. 4. Anisotropy of the Compton profiles for diamond: (a) $J_{100} - J_{110}$, (b) $J_{111} - J_{100}$. Theoretical curves have been convolved with experimental resolution function.

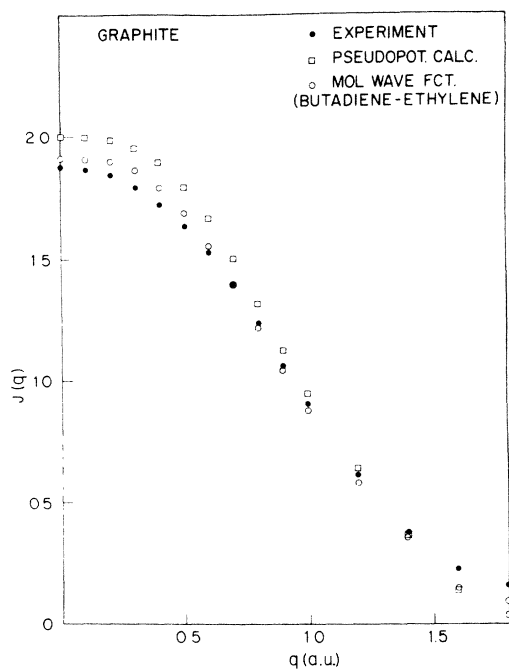


FIG. 5. Compton profiles for the valence electrons of graphite.

molecular approach gives better agreement than the pseudopotential method although the general features are present in both methods. The presence of the general features in both models indi-

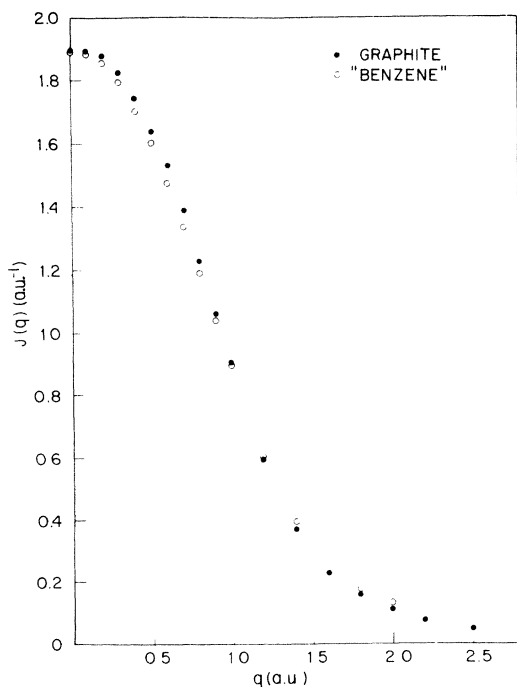


FIG. 6. Comparison of the Compton profiles of graphite and C-C bonds in benzene.

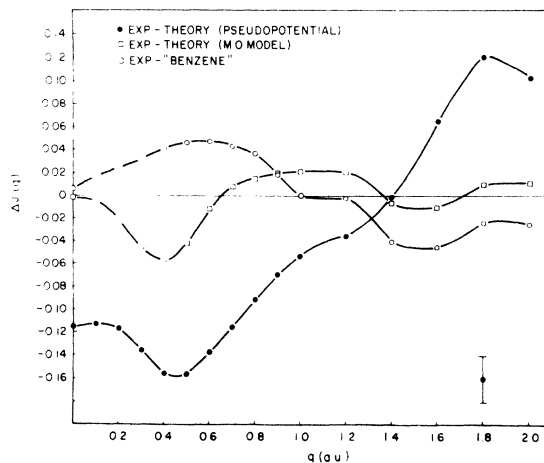


FIG. 7. Differences between the measured Compton profile in graphite and the profiles calculated from pseudopotential model, molecular orbital model, and the C-C bond in benzene.

cates that the anisotropy is mainly atomic or molecular in origin and not a property of the solid state. This is also supported by the striking similarity in $J(q)$ between benzene and graphite.

The first large peak in the theoretical anisotropy at $q \approx 0.5 \text{ a.u.}^{-1}$ may be due to the π bonding anisotropy along the c axis. The lattice constant along the c axis is 6.70 \AA and the distance between planes is 3.35 \AA , which correspond to momentum of 0.49 and 0.99 a.u. , respectively. It should be remembered that the molecular calculation completely ignores the interplane bonding, and the pseudopotential calculation is least accurate in this region because the wave function is very atomic-like. Thus the disagreement between both models and experiment may be attributed to the inaccurate treatment of the interplane bonding. The fact that the molecular calculation is slightly better is consistent with the atomic nature of the wave function in that region.

In Figs. 4(a) and 4(b) the pseudopotential and SCHF calculations for the anisotropy of diamond are compared with the experimental results. Note that for the $J_{100} - J_{110}$ anisotropy both theories agree well with each other and with experiment. This reaffirms the observations made in silicon⁵ that the $J_{100} - J_{110}$ anisotropy is insensitive to the details of the calculation and is basically a geometry effect. The $J_{111} - J_{100}$ anisotropy is, however, more sensitive because the $\langle 111 \rangle$ is the bonding direction. Here the two methods disagree considerably from each other and bracket the experimental results. Our criterion for agreement in this case is the quality of fit obtained in Si.⁶ The deviations are readily understood as the result of the two initial starting points for the calculations. The SCHF

calculation starts from a tight-binding model for the bond with atomiclike orbitals which tend to produce a large anisotropy in the bond. The pseudopotential calculation starts with a plane-wave expansion where the effects of the atomic potential create anisotropy. Thus the too small anisotropy calculated by the pseudopotential method and the too large anisotropy calculated by the SCHF method may be linked to the nature of their wave-function basis set.

The calculation of the average Compton profile by the pseudopotential method is 1.7% too high at $q=0$ because core-orthogonalization corrections have been omitted. The SCHF result¹² is about 4% too high at $q=0$. The cause of that discrepancy is not at the moment understood, since the anisotropy results indicate that $J(0)$ should be below the experimental value (i.e., more localized wave functions). It is, however, the same type of disagreement which the SCHF calculation found with measured x-ray form factors for diamond. The calculated form factors at (111) and (222) reciprocal-lattice vectors were too small, which means that the calculated charge distribution is more diffuse than the measured distribution. A more diffuse charge distribution of course gives a sharper Compton profile.

It is clear that the two previous arguments are in disagreement with each other. The SCHF Compton results indicate too large an anisotropy (more localized charge) while the SCHF x-ray form-factor results indicate too diffuse a charge distribution. The only superficial manner to reconcile the two is to insist that the spherical part of the wave function be more localized while the bonding part be more diffuse.

V. CONCLUSION

We find that the momentum density anisotropy for graphite calculated by either the pseudopotential method or a model using molecular wave functions is in qualitative but not quantitative agreement with experiment. We infer from this that the bonding in graphite is basically molecular in nature and the concept of a localized bond is reasonable. This contrasts with diamond, where it appears that solid-state effects are more significant and the localized-bond model is less accurate.

We also find that the different theoretical approaches considered are unable to provide ground-state wave functions for either diamond or graphite that accurately predict the measured anisotropy of the Compton profile.

For graphite this simply means we have not tried

the best theoretical methods. Pseudopotential calculations are known to give poorer results for the first-row elements due to the lack of p states in the core. The results of the molecular model calculations are perhaps more remarkable for the extent of their qualitative agreement than their quantitative disagreement.

For diamond the situation is more serious. Although the pseudopotential method suffers from the same problem we have already discussed for graphite, the SCHF calculations by Wepfer *et al.*¹² should in principle be more accurate. Unfortunately, their results for the Compton anisotropies agree no better with the measured anisotropies than do the pseudopotential results. It is quite possible that the calculation of Wepfer *et al.* can be improved since they find that changing their basis set shifts the one-electron energies by about 0.45 Ry.

It is also possible that even after improved calculations, the discrepancy will still exist. If this occurs, one possible source could be many-electron effects not accounted for in the Hartree-Fock approximation. Even though such effects should be small, they would make their major contribution in the momentum regions of interest. If they contributed an anisotropy as small as 1% in $J(q)$, they would markedly effect the measured anisotropy. The present difference between theory and experiment in diamond is about 2%.

One way to test the quality of Hartree-Fock molecular wave functions is to measure the momentum anisotropy in oriented crystals of small organic molecules. In these systems intermolecular interactions should be greatly reduced. Such a study is currently being performed.

As a result of the present study we are able to give partial answers to our original questions. Although band models have produced accurate Compton profiles for Si, the models considered are unsuccessful for the crystalline forms of carbon. Perhaps other calculational methods can do better. In answer to the second question we conclude that a localized bond model is sufficiently successful in both graphite and diamond to encourage further investigation of this model.

ACKNOWLEDGMENTS

We want to acknowledge the major contribution of T. A. Weber, who wrote the programs which compute Compton profiles from molecular wave functions. We also wish to thank L. F. Mattheiss for critically reading the manuscript.

¹L. Pauling, *J. Am. Chem. Soc.* **53**, 1367 (1931).

²J. C. Slater, *Phys. Rev.* **37**, 481 (1931).

³B. L. Hicks, *Phys. Rev.* **57**, 665 (1940).

⁴P. Eisenberger and W. C. Marra, *Phys. Rev. Lett.*

- 27, 1413 (1971).
- ⁵W. A. Reed and P. Eisenberger, Phys. Rev. B 6, 4596 (1972).
- ⁶K. C. Pandey, Bull. Am. Phys. Soc. 18, 323 (1973); K. C. Pandey (unpublished).
- ⁷L. C. Snyder and H. Basch, *Molecular Wave Functions and Properties* (Wiley, New York, 1972).
- ⁸M. Cooper and J. A. Leake, Philos. Mag. 15, 1201 (1967).
- ⁹R. J. Weiss and W. C. Phillips, Phys. Rev. 176, 900 (1968).
- ¹⁰J. Felsteiner, R. Fox, and S. Kahane, Phys. Lett. A 36, 442 (1970).
- ¹¹S. Berko, R. E. Kelly, and G. S. Plaskett, Phys. Rev. 106, 824 (1957).
- ¹²G. G. Wepfer, R. N. Euwema, G. T. Surratt, and D. L. Wilhite, Phys. Rev. (to be published).
- ¹³P. M. Platzman and H. Tzoar, Phys. Rev. 139, 410 (1965).
- ¹⁴P. Eisenberger and P. M. Platzman, Phys. Rev. 172, 415 (1970).
- ¹⁵P. Eisenberger and W. A. Reed, Phys. Rev. (to be published).
- ¹⁶P. Eisenberger and W. A. Reed, Phys. Rev. A 5, 2085 (1972).
- ¹⁷P. Eisenberger and W. A. Reed, Phys. Rev. (to be published).
- ¹⁸R. J. Weiss, W. C. Phillips, and A. Harvey, Philos. Mag. 17, 146 (1960).
- ¹⁹R. R. Haering and S. Mrozowski, *Progress in Semi-conductors* (Wiley, New York, 1960), Vol. 6; J. C. Slater, *Quantum Theory of Molecules and Solids* (McGraw-Hill, New York, 1965), Vol. 2; D. L. Greenaway, G. Harbeke, F. Bassani, and E. Tosatti, Phys. Rev. 178, 1340 (1969).
- ²⁰L. R. Saravia and D. Brust, Phys. Rev. 170, 683 (1968).
- ²¹W. Saslow, T. K. Bergstresser, and M. L. Cohen, Phys. Rev. Lett. 16, 354 (1966).
- ²²L. A. Hemstreet, C. Y. Fong, and M. L. Cohen, Phys. Rev. B 2, 2054 (1970).
- ²³W. van Haeringen and H. G. Junginger, Solid State Commun. 7, 1135 (1969).
- ²⁴W. van Haeringen and H. G. Junginger, Solid State Commun. 7, 1723 (1969).
- ²⁵A. O. E. Animalu and V. Heine, Philos. Mag. 12, 1249 (1965).
- ²⁶L. Cohen and V. Heine, in *Solid State Physics*, edited by F. Seitz *et al.* (Academic, New York, 1970), Vol. 24, p. 37.
- ²⁷K. C. Pandey and L. Lam, Phys. Lett. A 43, 319 (1973).
- ²⁸C. A. Coulson and R. Taylor, Proc. Phys. Soc. A 65, 815 (1952).
- ²⁹W. E. Duncanson and C. A. Coulson, Proc. Phys. Soc. A 65, 825 (1952).
- ³⁰R. W. Euwema, D. L. Wilhite, and G. T. Surratt, Phys. Rev. B 7, 818 (1973).
- ³¹G. T. Surratt, R. N. Euwema, and D. L. Wilhite, Phys. Rev. B 8, 4019 (1973).